BRD4 promotes p63 and GRHL3 expression downstream of FOXO in mammary epithelial cells

Sankari Nagarajan[1,†], Upasana Bedi[2,3,†], Anusha Budida[1], Feda H. Hamdan[1], Vivek Kumar Mishra[1], Zeynab Najafova[1], Wanhua Xie[1], Malik Alawi[4,5], Daniela Indenbirken[5], Stefan Knapp[6,7,8], Cheng-Ming Chiang[9], Adam Grundhoff[5], Vijayalakshmi Kari[1], Christina H. Scheel[10], Florian Wegwitz[1] and Steven A. Johnsen[1,*]

[1]Department of General, Visceral and Pediatric Surgery, Göttingen Center for Molecular Biosciences, University Medical Center Göttingen, 37077 Göttingen, Germany, [2]Institute of Molecular Oncology, University Medical Center Göttingen, 37077 Göttingen, Germany, [3]Institute of Tumor Biology, University Medical Center Hamburg-Eppendorf, 20246 Hamburg, Germany, [4]Bioinformatics Core, University Medical Center Hamburg-Eppendorf, 20251 Hamburg, Germany, [5]Heinrich-Pette-Institute, Leibniz Institute for Experimental Virology, 20251 Hamburg, Germany, [6]Structural Genomics Consortium, University of Oxford, Oxford OX3 7DQ, UK, [7]Target Discovery Institute, University of Oxford, Oxford OX3 7FZ, UK, [8]Institute for Pharmaceutical Chemistry, Goethe University Frankfurt 60323, Germany, [9]University of Texas Southwestern Medical Center, Simmons Comprehensive Cancer Center, Dallas, TX 75235, USA and [10]Institute of Stem Cell Research, Helmholtz Center for Health and Environmental Research Munich, 85764 Neuherberg, Germany

ABSTRACT

Bromodomain-containing protein 4 (BRD4) is a member of the bromo- and extraterminal (BET) domain-containing family of epigenetic readers which is under intensive investigation as a target for anti-tumor therapy. BRD4 plays a central role in promoting the expression of select subsets of genes including many driven by oncogenic transcription factors and signaling pathways. However, the role of BRD4 and the effects of BET inhibitors in non-transformed cells remain mostly unclear. We demonstrate that BRD4 is required for the maintenance of a basal epithelial phenotype by regulating the expression of epithelial-specific genes including *TP63* and *Grainy Head*-like transcription factor-3 (*GRHL3*) in non-transformed basal-like mammary epithelial cells. Moreover, BRD4 occupancy correlates with enhancer activity and enhancer RNA (eRNA) transcription. Motif analyses of cell context-specific BRD4-enriched regions predicted the involvement of FOXO transcription factors. Consistently, activation of FOXO1 function via inhibition of EGFR-AKT signaling promoted the expression of TP63 and GRHL3. Moreover, activation of Src kinase signaling and FOXO1 inhibition decreased the expression of FOXO/BRD4 target genes. Together,
our findings support a function for BRD4 in promoting basal mammary cell epithelial differentiation, at least in part, by regulating FOXO factor function on enhancers to activate *TP63* and *GRHL3* expression.

INTRODUCTION

Proper temporal regulation of transcription plays a major role in controlling lineage-specification and cancer progression (1). Among the various phases of transcription, elongation is an important rate–limiting step for many genes. During transcriptional elongation, RNA Polymerase II (RNAPII) is phosphorylated at serine 2 within its carboxy-terminal domain by Positive Transcription Elongation Factor-b (P-TEFb), which consists of Cyclin-Dependent Kinase 9 (CDK9) and Cyclin T1 or T2 (2). P-TEFb activity is tightly controlled by its reversible binding to HEXIM1 and 7SK snRNA, which inhibit its kinase activity (3). During transcriptional activation, P-TEFb is released from the inactive complex and can phosphorylate RNAPII and other target proteins.

Bromodomain-containing protein 4 (BRD4), a member of the BET (Bromodomain and Extra Terminal) family of proteins, functions to release P-TEFb from the inactive complex and facilitate its recruitment to chromatin, thereby promoting transcriptional elongation (4). Importantly, BRD4 binds to acetylated histones, mainly histone H4 acetylated at lysine residues 5, 8, 12 and/or 16 via its

two bromodomains, where its occupancy is associated with active transcription (5). In addition, BRD4 occupies distal enhancer regions where its presence is associated with enhancer activity and enhancer RNA (eRNA) transcription (6–9). Recent studies showed that BRD4-dependent gene expression programs are commonly dysregulated in various diseases including cancer (10). BRD4 function is highly context-dependent. Consistently, while we and others have reported positive roles for BRD4 in breast cancer cell proliferation, migration and metastasis (7,11–13), other studies suggest a tumor suppressor function of BRD4 (14,15). The mechanisms by which BRD4 functions in diverse normal cell types and the context-dependent determinants controlling its activity in different cellular contexts are largely unknown.

Epidermal Growth Factor Receptor (EGFR) and AKT signaling have been shown to promote epithelial dedifferentiation, epithelial-to-mesenchymal transition (EMT), migration and metastasis (16,17). EGFR mediates activation of AKT via Phosphoinositide-3 Kinase (PI3K) (18). The activation of AKT in turn leads to the phosphorylation and inactivation of the Forkhead box-containing transcription factor-O (FOXO1/3/4) family of proteins. FOXO proteins have been characterized as tumor suppressors and their expression is correlated with the maintenance of normal mammary epithelial acinar morphogenesis (19,20). Interestingly, a recent study revealed a cooperative function of FOXO1 and BRD4 in regulating *MYC* transcription to promote proliferation in Her2-positive breast cancer cells (21). Furthermore, molecular characterization of mammary basal cell-specific enhancer activation shows a significant involvement of enhancers located close to the *FOXO1* and *EGFR* genes (22). However, the epigenetic mechanisms controlling FOXO1 function in normal mammary cells is largely unclear. In this study, we show that BRD4 depletion or inhibition impairs epithelial differentiation by enhancer-associated regulation of the expression of the basal epithelium-specific gene *TP63* and the tumor suppressor gene *Grainy Head*-like transcription factor-3 (*GRHL3*). We also show that BRD4 colocalizes with FOXO factors on these enhancers and inhibition of EGFR/AKT signaling promotes the expression of *TP63* and *GRHL3*, while inhibiting FOXO1 leads to their downregulation.

MATERIALS AND METHODS

Cell culture

MCF10A cells were obtained from M. Oren (Weizmann Institute of Science, Israel) and MCF12A were purchased from the American Type Culture Collection (ATCC, USA). Both cell lines were grown in phenol red-free DMEM/F12 supplemented with 5% horse serum, 20 ng/ml epidermal growth factor, 0.1 µg/ml Cholera toxin, 10 µg/ml insulin, 0.5 µg/ml hydrocortisone, 100 units/ml penicillin and 100 µg/ml streptomycin at 37°C under 5% CO_2 (23). MDA-MB-231 cells were obtained from H. Wikman (University Hospital Center, Hamburg, Germany) and cultured in DMEM with high glucose and GlutaMAX supplemented with 10% fetal bovine serum (FBS), 100 units/ml penicillin and 100 µg/ml streptomycin. Primary cells from mouse

mammary epithelium were isolated from FVB-wild type female mice as previously described (24) with slight modifications to the protocol. These cells were grown in 1:1 DMEM/Ham's F12 mix supplemented with 10% FBS, 10 ng/ml EGF, 10 ng/ml Cholera toxin, 5 µg/ml pancreatic insulin, 100 units/ml penicillin and 100 µg/ml streptomycin at 37°C under 5% CO_2. HepG2 cells were obtained from M. Dobbelstein (University Medical Center, Göttingen, Germany) and grown in phenol red-free DMEM with 10% FBS, 1% sodium pyruvate, 100 units/ml penicillin and 100 µg/ml streptomycin at 37°C under 5% CO_2.

JQ1 was added to the cells for 2–3 days in the concentration of 250 nM and OTX015 (S7360, Selleckchem, USA) in the concentration of 500 nM. Perifosine (S1037, SelleckChem, USA) was added in the concentration of 10 µM for 24 h. FOXO1 inhibitor AS1842856 (344355, Calbiochem, EMD Millipore, USA) was used in the concentration of 100 nM and 1 µM as described (25) for 24 h after changing to media lacking EGF and Insulin for 48 h.

siRNA transfection

siRNA transfections were performed using Lipofectamine RNAiMAX (Invitrogen, USA) according to the manufacturer's instructions. The siRNAs utilized were siGENOME Non-targeting (Dharmacon; D-001206-13, GE Healthcare, USA) and BRD4 siRNAs (Dharmacon) with sequences 5′-GAACCUCCCUGA UUACUAU-3′, 5′-UAAAUGAGCUACCCACAGA-3′, 5′-UGAGAAAUCUGCCAGUAAU-3′ and 5′-AGCUGAACCUCCCUGAUUA-3′ for RNA sequencing. On target plus siRNAs (Dharmacon) were used for rest of the experiments: On target plus negative control (D-001810-02), BRD4 siRNAs with sequences 5′-AAACCGAGAUCAUGAUAGU-3′, 5′-CUACACG ACUACUGUGACA-3′, 5′-AAACACAACUCAAGC AUCG-3′, 5′-CAGCGAAGACUCCGAAACA-3′ and G RHL3 siRNAs (L-014017-02) with sequences 5′-GUAAA UAGCACUAACGAUC-3′, 5′-UGUAAGGCCUCUC GAGCAU-3′, 5′-GGAAGAUGCGCGAUGACGA-3′, 5′-CUAUCUAUGUAUUACGUCA-3′.

ChIP-sequencing and analyses

Chromatin immunoprecipitation was performed as described in supplementary information and as before (7,23). Published datasets were utilized for RNAPII under vehicle and tamoxifen-treated conditions from the Struhl laboratory (Harvard University) in MCF10A-ER-Src cells, H4K12ac (26) and GRO-sequencing from MCF10A (27), FOXO1 from human endothelial stromal cells (28) and BRD4 and H3K27ac from SUM159 cells (29). Published datasets from MCF7 cells were obtained for RNAPII (30), GRO-sequencing (31), H4K12ac (26), BRD4 (7), H3K4me3 (32), H3K4me1 and H3K27ac (33).

MCF10A and MCF7-specific BRD4- and RNAPII-bound distal enhancers were identified using DiffBind analyses (34). The regions were selected with the cut-off of 2-fold higher binding with FDR ≤ 0.05. Motif analysis was performed using oPOSSUM 3.0 (35). For motif analysis, MCF10A- or MCF7-specific BRD4-bound broad-peaks from MACS2 were intersected with RNAPII-bound

broadpeaks and then with RNAPII narrowpeaks. MCF7-specific BRD4-enriched regions were used as background sequences for finding MCF10A-specific motifs and vice-versa. JASPAR core profiles were used as motif database. Genes proximal to the enhancers were identified by GREAT analyses (36) using 'Basal plus extension' method where each genomic region is overlapped with genes which are 5kb upstream and 1 kb downstream (proximal), plus up to 1000 kb (distal).

RNA-sequencing (RNA-seq) and data analysis

The high-throughput RNA-seq library preparation and data analysis were performed as described (7). Briefly, libraries were generated from 500 ng of total RNA using the TruSeq RNA Sample Preparation Kit (Illumina, Cat.No. RS-122-2002, USA). Accurate quantitation of cDNA libraries was performed using the QuantiFluor™ dsDNA System (Promega, USA). The size range of final cDNA libraries was determined using a DNA 1000 chip on the Bio-analyzer 2100 from Agilent (280 bp). cDNA libraries were amplified and sequenced by using the cBot and HiSeq2000 from Illumina (SR; 1×50 bp; 51 cycles with single indexing; 6GB ca. 30–35 million reads per sample).

Sequence reads were aligned to the human reference assembly (UCSC version hg19) using Bowtie 2.0 (37). For each gene, the number of mapped reads was counted and DESeq (38) was used to analyze the differential expression. Gene Set Enrichment Analysis was performed with GSEA (39). Pathways were retrieved from Molecular Signature database (MSigdb) (40). Pathway datasets are referred to as follows: BOSCO_EPITHELIAL_DIFFERENTIATION_MODULE (41), MANALO_HYPOXIA_DN (42), WONG_EMBRYONIC_STEM_CELL_CORE (43), CROMER_TUMORIGENESIS_DN (44), SOTIRIOU_BREAST_CANCER_GRADE_1_VS_3_UP (45), LIN_SILENCED_BY_TUMOR_MICROENVIRONMENT (46), JAEGER_METASTASIS_DN (47), ODONNELL_METASTASIS_DN (48), CHARAFE_BREAST_CANCER_BASAL_VS_MESENCHYMAL_UP (49). The significant pathways were selected according to FDR value ≤ 0.05. Gene ontology analyses were performed using default conditions in DAVID (**D**atabase for **A**nnotation, **V**isualization and **I**ntegrated **D**iscovery - v6.7) (50) and the significant pathways (FDR ≤ 0.05) were shown.

Gene groups according to the expression levels in MCF10A were made based on the log2 average values of each gene from RNA sequencing data after normalization with DESeq (38) under thresholds: NO refers to the genes with $\log_2$ average values equal to; LOW refers to the genes with values of $0 < \log_2$ average ≤ 5; MIDDLE refers to the genes with values of $5 < \log_2$ average ≤ 8; HIGH refers to the genes with values of $8 < \log_2$ average ≤ 10; VERY_HIGH refers to the genes with values of $\log_2$ average >10. To get 'Up', 'Down' and 'Non' classes mentioned in Supplementary Figure S4D, the thresholds were used as average fold change (after JQ1 treatment compared to control cells) ≥ 2 ('Up') and average fold change ≤ 0.5 ('Down') with adjusted P-values ≤ 0.05. Non (unchanged) genes – 0.99–1.05 Fold change, p-value > 0.05.

Microarray datasets from MCF10A-ER-SRC (51) were analyzed using MAS5 function in the Bioconductor Affy package to remove the noise and for normalization (52). Genes downregulated after 36 h of Tamoxifen treatment were identified with average fold change ≤ 0.667 with p-values ≤ 0.05. These genes were used to make the gene set for GSEA analysis and labeled as MCF10A-ER-SRC-TAM36HR-DOWN. Differentially regulated genes from p63 overexpression and knockdown in MCF10A cells were obtained from (53) and 1.5-fold up- (average fold change $\geq$ 1.5) or downregulated (average fold change ≤ 0.667) genes were used for making the gene sets with q-value ≤ 0.05. Genes within a custom-made gene set were sorted according to their extent of regulation representing the pathway or function. For p63 regulation after JQ1 treatment in triple-negative breast cancers, normalized counts were obtained by DESeq analyses of the published dataset (29).

Statistical analyses

ANOVA single factor analyses was used to calculate the p-value for qPCR-based analyses. For ChIP-seq and RNA-seq analyses, q-value (to call peaks) and adjusted p-value of ≤ 0.05 was considered for statistical significance respectively. Motif analyses were performed using oPOSSUM 3.0 and Z-score and Fisher score (negative natural logarithm of p-value) were utilized for showing significant motifs. Enrichment score and normalized enrichment score were shown for GSEA analyses with FDR q-value ≤ 0.05. Wilcoxon rank-sum test was used to find p-values for median values to denote the significance for box plots.

RESULTS

BRD4 promotes the expression of epithelial gene signatures

To investigate the importance of BRD4 in non-transformed mammary epithelial cells, we performed siRNA-mediated knockdown or inhibition of BRD4 by the small molecule inhibitors (*S*)-JQ1 (active stereoisomer) and OTX015 in MCF10A and MCF12A (normal basal-like mammary epithelial) cells. RNA-sequencing analyses in MCF10A cells revealed that BRD4 depletion or inhibition with JQ1 had a similar effect on gene expression even though JQ1 inhibits the entire family of BET proteins including BRD2, 3 and 4 (Figure 1A, see also Supplementary file 1). Using Gene Set Enrichment Analyses (GSEA) and DAVID gene ontology analyses (54,50), gene expression signatures associated with epithelial differentiation and EMT were shown to be significantly enriched in control conditions compared to BRD4 perturbation (Figure 1B and Supplementary Figure S1A–D). The expression of several genes involved in the suppression of metastasis (*IL1RN*) (55), epithelial phenotype (*KRT13*, *KRT15*, *CEACAM1*) and an epithelium and stem cell differentiation-specific ETS family transcription factor, E74-like factor 3 (*ELF3*) (46,56) were all confirmed to be significantly downregulated upon BRD4 knockdown or treatment with the BET bromodomain inhibitors JQ1 or OTX015 in both MCF10A and MCF12A cell lines (Figure 1C and D, Supplementary Figure S1E and S1F). Together, these results suggest that BRD4 is required for the expres-
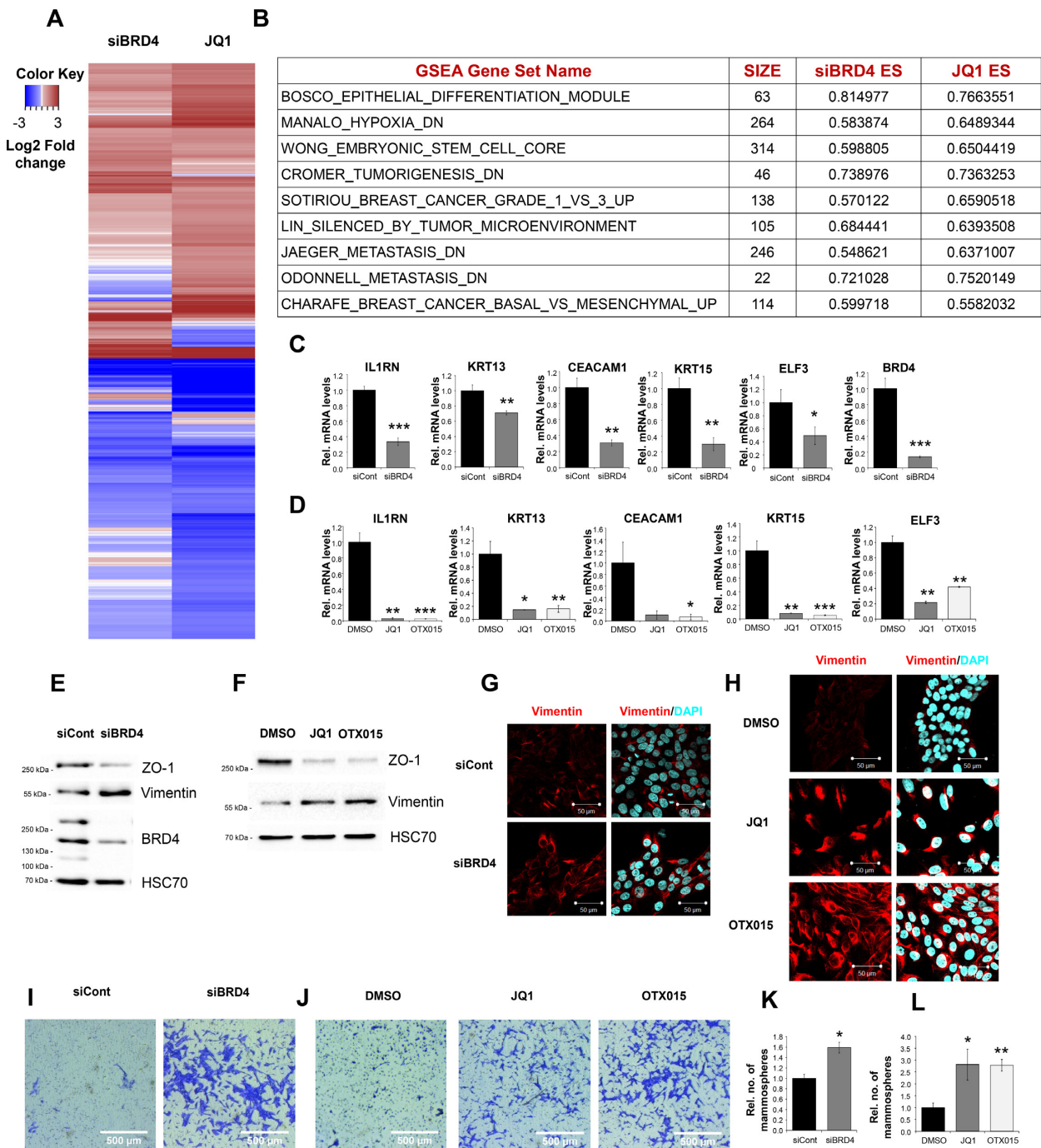
Figure 1. BRD4 is required for epithelial-specific gene expression and cellular phenotype. MCF10A cells were transfected with siRNAs for negative control (siCont), BRD4 (siBRD4) or treated with JQ1 or OTX015 for 3 days. (**A**) Heatmap analysis showing the differentially regulated genes by mRNA sequencing. Gene expression values in treated conditions were normalized to reads from cells transfected with control siRNA. Heatmap was generated from significant (*p*-values calculated by Benjamini and Hochberg test ≤ 0.05) up- (brown) or down- (blue) regulated genes with the cut-off of -1.0 and $+ 1.0$ $\log_2$ fold change values in one of the conditions; $n = 2$. (**B**) GSEA analyses showing enriched pathways on control conditions compared with BRD4 perturbation. ES—enrichment score. FDR ≤ 0.05. (C and D) Epithelial genes regulated by BRD4 siRNA (**C**) and JQ1 or OTX015 (**D**) were confirmed by qPCR and denoted as 'Rel. mRNA levels' which is normalized to *RPLP0* expression levels and the control condition. Data are represented as mean $\pm$ standard deviation. $n = 3$. ***$P \leq 0.001$, **$P \leq 0.01$, *$P \leq 0.05$. (E and F) Knockdown of BRD4 (**E**) or JQ1/OTX015 treatment (**F**) results in decreased expression of the epithelial marker ZO-1 and an increase in mesenchymal marker Vimentin as shown by Western blot analyses of whole cell protein lysates. BRD4 knockdown efficiency is verified by BRD4 antibody and all isoforms are shown along with the molecular weight in kilodaltons (kDa). HSC70 is used as a loading control. (G and H) Immunofluorescence staining of Vimentin following BRD4 knockdown (**G**) or JQ1/OTX015 treatment (**H**) confirms a decreased epithelial phenotype. DAPI staining shows the nucleus. Scale bar represents 50 μm. (I and J) Trans-well migration assay with crystal violet staining indicates increased migration upon BRD4 knockdown (**I**) or JQ1/OTX015 treatment (**J**). Scale bar represents 500 μm. (K and L) Quantification of mammospheres showed an increase with BRD4 knockdown (**K**) or JQ1/OTX015 treatment (**L**). The values were normalized to the control and represented as 'Rel. no. of mammospheres'. Data are represented as mean $\pm$ standard deviation. $n = 3$.

sion of epithelial genes in non-transformed basal-like mammary epithelial cells.

Consistent with a decreased epithelial cell phenotype, our results revealed that BRD4 perturbation leads to downregulation of the protein levels of the epithelial-specific tight junction marker ZO-1 and the upregulation of a mesenchymal marker Vimentin (Figure 1E–H, Supplementary Figure S1G and S1H). Furthermore, upon BRD4 perturbation, cells displayed an increased capacity for migration and mammosphere formation (Figure 1I–L, Supplementary Figure S1I–L). Together, these results support a role for BRD4 in the maintenance of an epithelial gene expression program.

BRD4 regulates epithelial gene expression and suppresses stem cell-like characteristics in part by promoting the expression of *GRHL3*

To further elucidate the mechanism by which BRD4 promotes epithelial characteristics, we closely examined the BRD4-dependent genes. Interestingly, the expression of *GRHL3*, a tumor suppressor and a transcription factor belonging to the *Grainyhead*-like family, which have been reported to regulate epidermal integrity, EMT and MET (57,58), was found to be significantly downregulated following BRD4 knockdown or inhibition (Figure 2A–D, Supplementary Figure S2A–D). Consistent with being a central target of BRD4 in controlling epithelial cell phenotype, our studies showed that GRHL3 depletion partially mimicked the effect of BRD4 perturbation and resulted in decreased ZO-1 and increased Vimentin expression, as well as increased migration and mammosphere formation (Figure 2E–H, Supplementary Figure S2E–I). Moreover, we observed that the expression of epithelial genes downregulated following BRD4 perturbation was also partially downregulated by *GRHL3* knockdown (Figure 2I), suggesting that the effects observed in response to BRD4 perturbation may, at least in part, be mediated via decreased *GRHL3* expression.

BRD4 promotes p63 expression and its transcriptional signature

The p63 protein encoded by the *TP63* gene plays a central role in epithelial development, basal cell-specific gene expression and survival (59–61,22). p63 has two major isoforms, a longer form containing an amino-terminal transactivation domain (TAp63) and a shorter form lacking the transactivation domain (ΔNp63). Consistent with the role of BRD4 in maintaining basal mammary epithelial cell phenotype, our RNA-seq analyses identified *TP63* to be significantly downregulated by BRD4 perturbation in MCF10A cells. As reported previously (53), MCF10A and MCF12A cells have increased levels of ΔNp63 and comparatively low levels of TAp63. We observed that both transcripts were significantly downregulated by BRD4 perturbation (Figure 3A–H, Supplementary Figure S3). In order to determine whether this regulation is a feature common to basal-like mammary epithelial cells, we isolated primary mouse mammary epithelial cells and observed that BRD4 inhibition resulted in decreased levels of total and isoform-specific *Trp63*

expression (Figure 3I–J). These findings were further supported by the analysis of published RNA-seq datasets from triple negative breast cancer cells (TNBC) (29), where these effects were also seen for the TNBC cell line SUM159, further supporting that *TP63* expression is generally dependent upon BRD4 function in basal-like mammary epithelial and breast cancer cells (Figure 3K). Notably, MCF7 cells, a luminal-like epithelial breast cancer cell line, do not express p63. However, another triple negative basal-like breast cancer cell line MDA-MB-231 also showed JQ1 concentration-dependent downregulation of p63 (Supplementary Figure S3E). Consistent with a role for p63 downregulation in eliciting the effects observed following BRD4 perturbation, JQ1-downregulated genes were highly enriched in published gene sets that were downregulated following p63 knockdown or upregulated by p63 overexpression (53) (Figure 3L and M). Together, these findings support a role for BRD4 in promoting p63 expression and subsequent p63-dependent gene regulation in various basal-like mammary and breast cancer cells.

BRD4 occupies potential enhancer regions of epithelial genes and is associated with enhancer activity

To understand the mechanism behind the role of BRD4 in promoting epithelial-related gene expression, we performed chromatin immunoprecipitation sequencing (ChIP-seq) analyses for BRD4. In agreement with our RNA-seq analyses, Genomic Regions Enrichment of Annotations Tool (GREAT) analyses (36) on BRD4-enriched regions revealed an association of BRD4 with various EMT, breast cancer and p63-related pathways (Figure 4A and Supplementary Figure S4A). Notably, approximately 80% of BRD4-enriched regions were located distal to transcription start sites (TSS), supporting the previously described role of BRD4 at enhancers (Figure 4B, Supplementary Figure S4B) (6,7,9). In general, BRD4 occupancy correlated with gene expression where moderate and highly expressed genes were generally more sensitive to JQ1 (Figure 4C, Supplementary Figure S4C and D).

Consistent with a primary function at distal regulatory elements, the occupancy of BRD4 and H4K12ac at potential enhancer regions were closely associated with the occupancy of the active enhancer marks H3K4me1 and H3K27ac (Figure 4D and E, Supplementary Figure S4E and S4F). As we previously reported in an estrogen receptor-dependent context (7,26), putative BRD4-bound enhancer regions (BRD4$^+$/H3K4me1$^+$/H3K27ac$^+$/H3K4me3$^-$) displayed significant RNAPII occupancy and produced nascent RNA transcripts, indicative of eRNA production. This correlation was also observed on the distal enhancers of the epithelial-related BRD4 targets *TP63*, *GRHL3*, *ELF3* and *IL1RN* (Figure 4F and G, Supplementary Figure S4G and S4H). Notably, around 38% of Molecular Signature Database (40) (MolSigDB)-defined EMT-related genes possess potential enhancer-specific BRD4 occupancy, suggesting a direct role for BRD4 in their regulation (Supplementary Figure S4I). Interestingly, pathway analyses on distal BRD4-enriched regions displaying enhancer-like characteristics revealed a significant enrichment of p63-
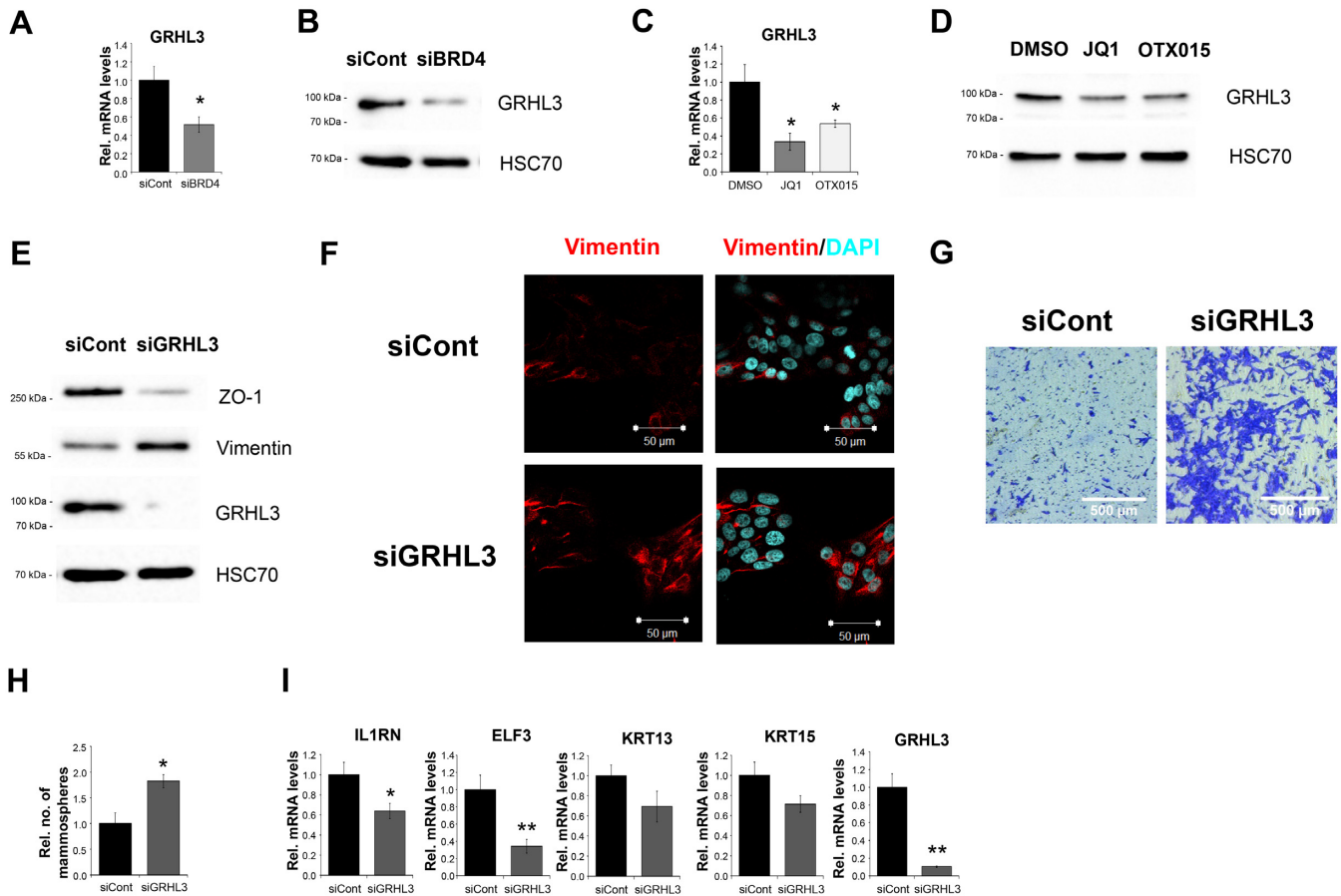
Figure 2. BRD4 regulates GRHL3 expression and affects epithelial phenotype. (A and C) *GRHL3* expression is decreased by following BRD4 siRNA transfection (**A**) or JQ1/OTX015 treatment (**C**) in MCF10A cells as confirmed by qPCR and expressed as 'Rel. mRNA levels'. Data are represented as mean ± standard deviation. $n = 3$. *$P \leq 0.05$. (**B** and **D**) Western blot analyses of whole cell protein lysates showing downregulation of GRHL3 after BRD4 siRNA (B) or JQ1/OTX015 treatment (**D**) in MCF10A cells. (**E**) Knockdown of GRHL3 (siGRHL3) results in decreased expression of the epithelial marker ZO-1 and an increase in the mesenchymal marker Vimentin as verified by Western blot analysis of whole cell protein lysates. GRHL3 knockdown efficiency was confirmed using a GRHL3 antibody. (**F**) Immunofluorescence staining of Vimentin following GRHL3 knockdown. Scale bar represents 50 μm. (**G**) Trans-well migration assay stained with crystal violet indicates an increase in migration upon GRHL3 knockdown. Scale bar represents 500 μm. (**H**) Quantitation of mammospheres formed showed an increase after GRHL3 knockdown. Data are represented as mean ± standard deviation. $n = 3$. *$P \leq 0.05$. (**I**) Epithelial genes regulated by GRHL3 siRNA were confirmed by qPCR and denoted as 'Rel. mRNA levels'. Data are represented as mean ± standard deviation. $n = 3$. **$P \leq 0.01$, *$P \leq 0.05$.

and integrin signaling-related transcriptional signatures associated with basal cell survival and tumor invasiveness (Supplementary Figure S4J) (62,63).

BRD4 promotes RNAPII recruitment and enhancer RNA transcription near *TP63* and *GRHL3* Genes

In order to investigate the mechanisms by which BRD4 regulates p63 and GRHL3 expression, we next examined the binding profiles of BRD4, RNAPII and histone acetylation occupancy near *TP63* and *GRHL3*. ChIP analyses of BRD4 and RNAPII occupancy revealed that decreased BRD4 occupanc on enhancers in response to JQ1 or OTX015 treatment leads to a significant concomitant reduction in RNAPII occupancy on these regions (Figure 4H, I and K, L). While BRD4 occupancy was not significantly affected around the ΔNp63 TSS, the potential enhancers displayed a substantial reduction in the occupancy of both BRD4 and RNAPII (Figure 4H and I). In contrast to *TP63*, RNAPII occupancy near the *GRHL3* TSS

was not appreciably affected by BRD4 inhibition. However, we did observe a downregulation of non-spliced heterogeneous RNA (hn*GRHL3*) by BRD4 inhibition, supporting a role for BRD4 in the regulation of *GRHL3* gene transcription (Figure 4M). Most importantly, BRD4 inhibition resulted in the downregulation of the putative *TP63*- and *GRHL3*-associated eRNAs (Figure 4J and N). Altogether, these studies demonstrate an enhancer-associated function of BRD4 in modulating the expression of *TP63* and *GRHL3*.

BRD4 associates with FOXO factors on cell-specific enhancers

We next performed differential binding analyses (34) to define distal BRD4-enriched regions which are highly specific to MCF10A in comparison to MCF7 cells (7) to identify lineage-specific enhancers potentially important for basal epithelial differentiation compared to luminal epithelial cells. Consistent with a cellular context-dependent func-
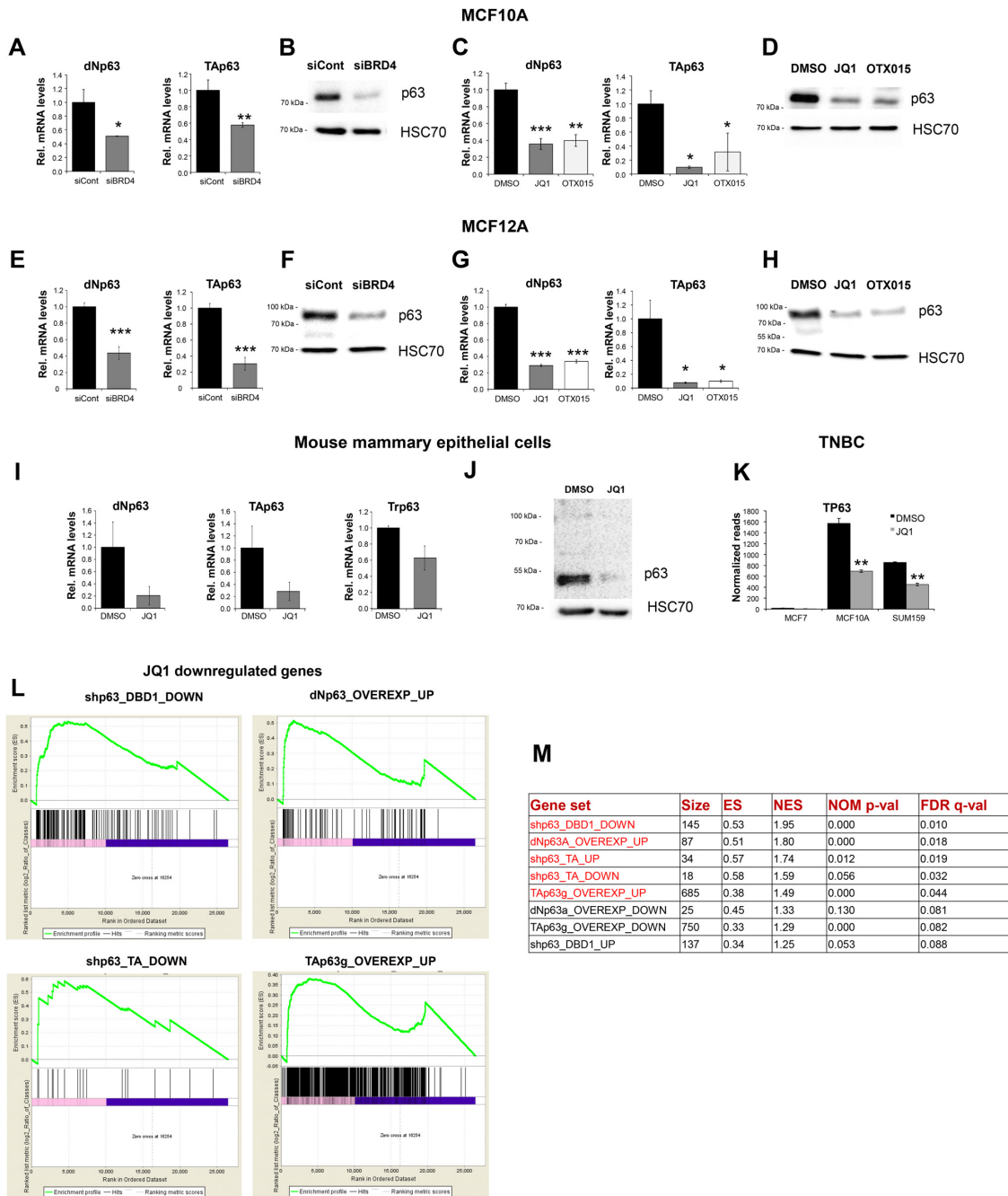
Figure 3. BRD4 promotes p63 expression and p63-dependent gene expression programs in basal-like epithelial cells. (A, C, E, G) ∆Np63 (dNp63) and TAp63 expression is decreased following BRD4 siRNA transfection (**A** and **E**) or JQ1/OTX015 treatment (**C** and **G**) in MCF10A (A and C) and MCF12A cells (E and G) as confirmed by qPCR and denoted as 'Rel. mRNA levels'. Data are represented as mean ± standard deviation. $n = 3$. ***$P ≤ 0.001$, **$P ≤ 0.01$, *$P ≤ 0.05$. (B, D, F and H) Western blot analyses of MCF10A (**B** and **D**) and MCF12A (**F** and **H**) protein lysates showing downregulation of p63 (ca. 70 kDa band shown) after BRD4 siRNA (B and F) or JQ1/OTX015 treatment (D and H). Molecular weight is shown in kilodaltons (kDa). (**I**) ∆Np63 (dNp63), TAp63 and total *Trp63* expression was also regulated by JQ1 treatment in mouse primary mammary epithelial cells as confirmed by qPCR and denoted as 'Rel. mRNA levels'. Data are represented as mean ± standard deviation. $n = 2$. (**J**) Western blot analyses of protein lysates from mouse primary mammary epithelial cells showing a downregulation of total p63 after JQ1 treatment. (**K**) Normalized read counts of total *TP63* expression with JQ1 treatment in the ER-positive luminal breast cancer cell line MCF7, normal basal epithelial cell line MCF10A and the triple-negative breast cancer cell line SUM159. Data are represented as average normalized reads ± standard deviation. $n = 2$. (**L**) GSEA analyses showing enrichment plots comparing JQ1 downregulated genes with the gene sets downregulated upon loss of ∆Np63 (shp63_DBD1_DOWN) and TAp63 (shp63_TA_DOWN) or upregulated genes upon overexpression of ∆Np63 (dNp63_OVEREXP_UP) and TAp63 (TAp63g_OVEREXP_UP). JQ1 downregulated genes were arranged with log2 fold changes in ascending order. ES—enrichment score. FDR ≤ 0.05. (**M**) Table showing the results from GSEA with enrichment scores comparing JQ1 downregulated genes with the gene sets up- or downregulated upon loss of ∆Np63 (shp63_DBD1_UP, shp63_DBD1_DOWN) and TAp63 (shp63_TA_UP, shp63_TA_DOWN) or up- or downregulated genes upon overexpression of ∆Np63 (dNp63_OVEREXP_UP, dNp63_OVEREXP_DOWN) and TAp63 (TAp63g_OVEREXP_UP, TAp63g_OVEREXP_DOWN). Size—number of genes in the gene set, NES—normalized enrichment score, NOM *p*-val—nominal *p*-value, FDR *q*-val—false discovery rate.
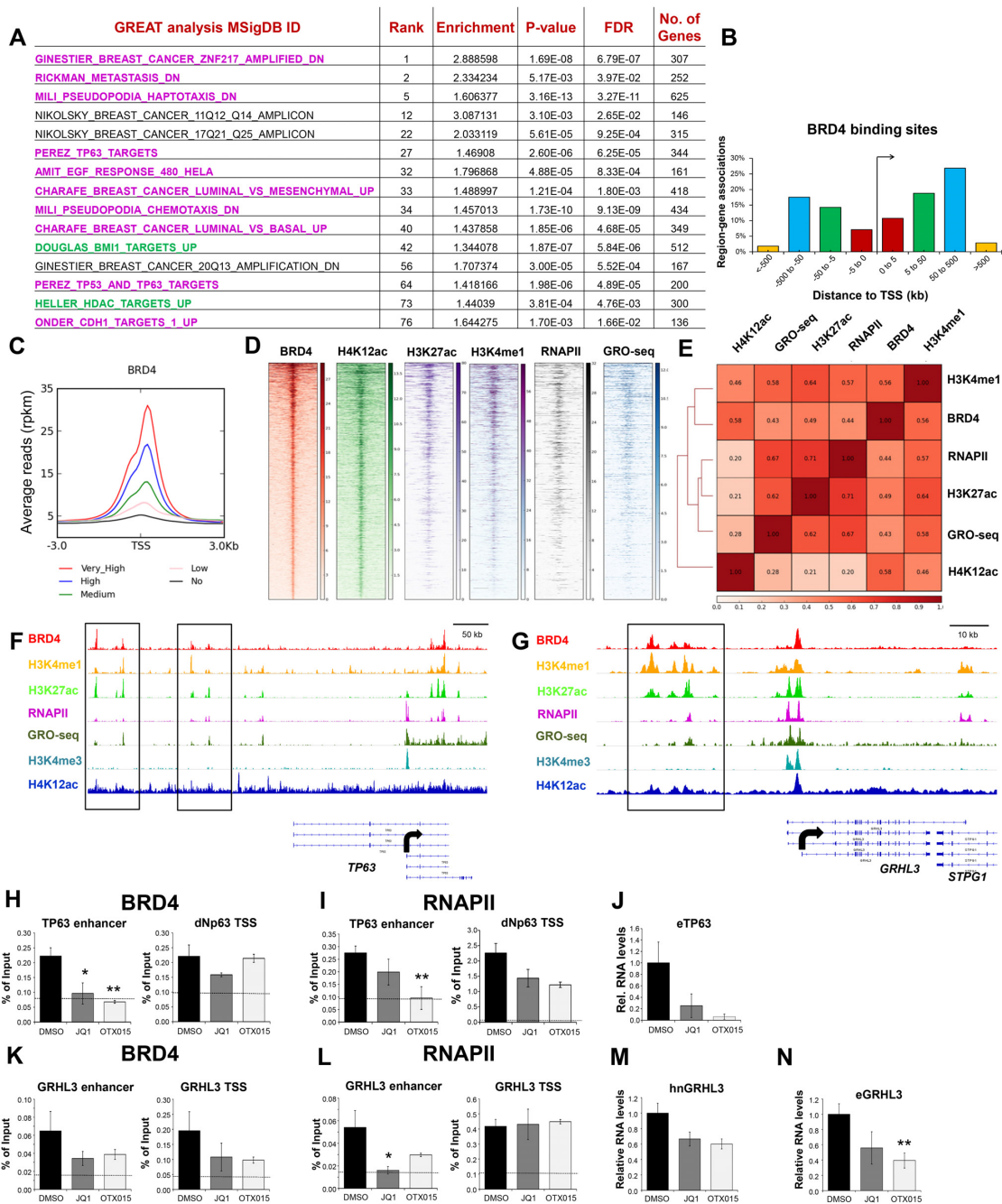
Figure 4. BRD4 occupancy correlates with enhancer activity and eRNA transcription near *TP63* and *GRHL3*. (**A**) GREAT analysis on BRD4-occupied regions identified numerous EMT and breast cancer-related pathways (highlighted in purple). Other epigenetic pathways are highlighted in green. *P*-value and FDR ≤ 0.05. (**B**) Distribution of BRD4 occupancy shown in percentage and as the distance from TSS (arrow mark) in kilobases (kb). (**C**) Average profiles showing the BRD4 occupancy correlating with the level of gene expression. Genes were grouped according to the normalized rpkm values of gene expression as 'Very_High', 'High', 'Medium', 'Low' and 'No'. The plot shows the average normalized RPKM values of BRD4 occupancy. TSS ± 3 kb is shown. Standard error is included as a shade on the plot. (D, E) Heatmap (**D**) and correlation (**E**) analyses depicting the occupancy of BRD4, H4K12ac, H3K27ac, H3K4me1, RNAPII and enhancer RNA transcription shown by global run on sequencing (GRO-seq) located on distal BRD4 occupied regions aligned according to its maximum signal of BRD4 occupancy. Scale is shown as normalized RPKM values for heatmap. Regions ± 5 kb is shown. Spearman correlation coefficient values are shown in the correlation plot. (F and G) Occupancy profiles of BRD4, H4K12ac, H3K27ac, RNAPII and enhancer RNA transcription shown by global run on sequencing (GRO-seq) on the distal regions of *TP63* (**F**) and *GRHL3* (**G**). Active transcriptional start sites and the direction of transcription are indicated by black arrows. Scale bar is denoted in kilobases. (H, I, K, L) ChIP analyses of BRD4 (**H**, **K**) and RNAPII (**I**, **L**) occupancy on *TP63* (H and I) and *GRHL3* (K and L) enhancer and TSS regions after JQ1/0TX015 treatment. Immunoprecipitated DNA was normalized to the input and denoted in percentage. Black dotted line denotes the background DNA precipitated by a negative control IgG. Data are represented as mean ± standard deviation. *n* = 3. **P ≤ 0.01, *P ≤ 0.05. (**M**) Regulation of nascent heterogeneous nuclear RNA expression of *GRHL3* (hnGRHL3) by JQ1/0TX015 treatment was confirmed by qPCR and denoted as 'Rel. RNA levels'. Data are represented as mean ± standard deviation. *n* = 3. (J and N) Regulation of enhancer RNA expression of *TP63* (eTP63) (J) and *GRHL3* (eGRHL3) (N) by JQ1/0TX015 treatment was confirmed by qPCR and denoted as 'Rel. RNA levels'. Data are represented as mean ± standard deviation. *n* = 3. **P ≤ 0.01.

tion of BRD4, we observed significant differences in the occupancy of BRD4 in these two different cell systems (Figure 5A, Supplementary Figure S5A–F). At least 1490 distal regions were found to possess differential binding of BRD4 (Supplementary Figure S5C). Overall, MCF7 cells show more differentially enriched regions displaying higher occupancy of BRD4 in comparison to MCF10A (Supplementary Figure S5D). As expected based on our previous results (7), regions specific to MCF7 display significant ERα binding, which is not observed for MCF10A-specific sites (Supplementary Figure S5G). This further supports a context-specific function of BRD4 and relationship with lineage-specific transcription factors. Consistent with MCF10A cells displaying a basal-like gene expression signature, MCF10A-specific sites showed similarity to the basal-like breast cancer cell line SUM159 for BRD4 and H3K27ac occupancy (Figure 5A). Importantly, heatmap analyses demonstrated the cell line-specific occupancy of active enhancer marks with eRNA transcription at these 1490 regions (Figure 5A). Pathway analyses on MCF10A-specific BRD4-bound distal regions showed a significant association with integrin-, EGF-, basal- and metastasis-related pathways (Figure 5B, Supplementary Figure S5H). SUM159 and MCF10A showed similar BRD4 occupancy on potential enhancers around *TP63*, while MCF7 displayed background signal, further confirming the context-specific occupancy of BRD4 on *TP63* enhancers (Figure 5C).

In order to identify transcription factors potentially mediating BRD4 recruitment to these regions, we performed motif analyses on RNAPII peaks contained within MCF7- or MCF10A-specific BRD4-enriched regions. As anticipated from our previous work (7), MCF7-specific RNAPII/BRD4-occupied distal regions displayed an enrichment of ERα and forkhead motifs (Supplementary Figure S5I). Interestingly, MCF10A-specific RNAPII-bound regions also showed an association of several similar forkhead motifs (Supplementary Figure S5J). Consistent with the association of FOXO-, Insulin-, EGF-related pathways with enhancer-specific BRD4 binding (Figure 5B, Supplementary Figure S4J and S5H), we also found that 44% of the MCF10A-specific RNAPII/BRD4-bound regions showed a significant enrichment of a FOXO3 motif (Figure 5D and E). Furthermore, pathway analyses on these regions revealed a significant association with EGF- and PI3K-related pathways (Supplementary Figure S5K–M) as well as integrin-related pathways (Supplementary Figure S5L), which have been reported to function downstream of PI3K signaling (62,64). Altogether, these results suggest that MCF10A-specific enhancer-associated BRD4 occupancy may functionally interact with EGF/PI3K/FOXO signaling to regulate basal epithelium-specific gene expression, consistent with the role of *FOXO1* and *EGFR* enhancer activation in mammary basal epithelial cell growth (22).

Src activation decreases RNAPII occupancy on BRD4 targets

To further validate the association of BRD4 and FOXO activity, we utilized published RNAPII ChIP-seq data from MCF10A-ER-Src cells where administration of Tamoxifen results in the activation of Src and subsequent downstream signaling proteins including AKT. Heatmap and aggregate plot analyses showed that TSS regions of BRD4 target genes display minimal but significant decreases in RNAPII occupancy after Src activation (Figure 6A and B, Supplementary Figure S6A and S6B). This effect was more pronounced at MCF10A-specific BRD4 bound distal regions where RNAPII occupancy was more strongly decreased in response to Src activation (Figure 6C and D), supporting a mechanism whereby the enhancer-specific association of RNAPII and BRD4 is inhibited by activation of Src-dependent signaling. We also performed differential binding analyses for RNAPII occupancy in vehicle- and Tamoxifen-treated conditions on regions surrounding MCF10A-specific BRD4-bound putative enhancers (Supplementary Figure S6C–F). Consistently, pathway analyses on the regions displaying higher occupancy of RNAPII under vehicle conditions compared to Tamoxifen also showed an enrichment of integrin-, FOXO-, EGF-, basal and EMT-related pathways (Figure 6E and F, Supplementary Figure S6G and S6H). Genes associated with these regions were identified by GREAT analysis and displayed a significant overlap with genes proximal to FOXO3 motif-containing MCF10A-specific BRD4-bound distal regions (Figure 6G). Further confirmation of the interconnectivity between Src signaling and BRD4 function was provided by GSEA studies demonstrating a specific enrichment of genes downregulated following by BRD4 inhibition or depletion in gene sets downregulated by Src activation 51 (Figure 6H). Together these results suggest that Src activation leads to the downregulation of MCF10A-specific BRD4 target gene expression via affecting RNAPII occupancy at distal BRD4-enriched enhancers.

AKT-FOXO1 signaling regulates p63 and GRHL3 expression

In order to further establish the relationship between BRD4 and EGF/AKT/FOXO signaling, we utilized a published ChIP-seq dataset for FOXO1 from human endometrial stromal cells (28). Interestingly, despite this dataset being from a heterologous system, BRD4-bound enhancers near both the *TP63* and *GRHL3* genes showed significant occupancy of FOXO1 (Figure 7A and B). Notably, many of these sites, as well as the TSS, also showed decreased RNAPII occupancy following Src activation.

The standard growth conditions for MCF10A and MCF12A cells include the addition of both EGF and insulin, which are known activators of PI3K/AKT signaling. Thus, we examined whether the removal of EGF and Insulin from the growth medium or the addition of the AKT inhibitor Perifosine would affect the expression of *TP63* and *GRHL3*. Indeed, both conditions significantly increased the gene expression levels and JQ1 treatment downregulated their induced expression (Figure 7C and D). In order to test whether BRD4 activity is generally required for FOXO activity, we also examined the effects of BET inhibition on the HepG2 hepatoma cell line, where FOXO1 signaling controls glucose and lipid metabolism (65–68). Consistent with a general role for BRD4 in mediating FOXO-dependent

A
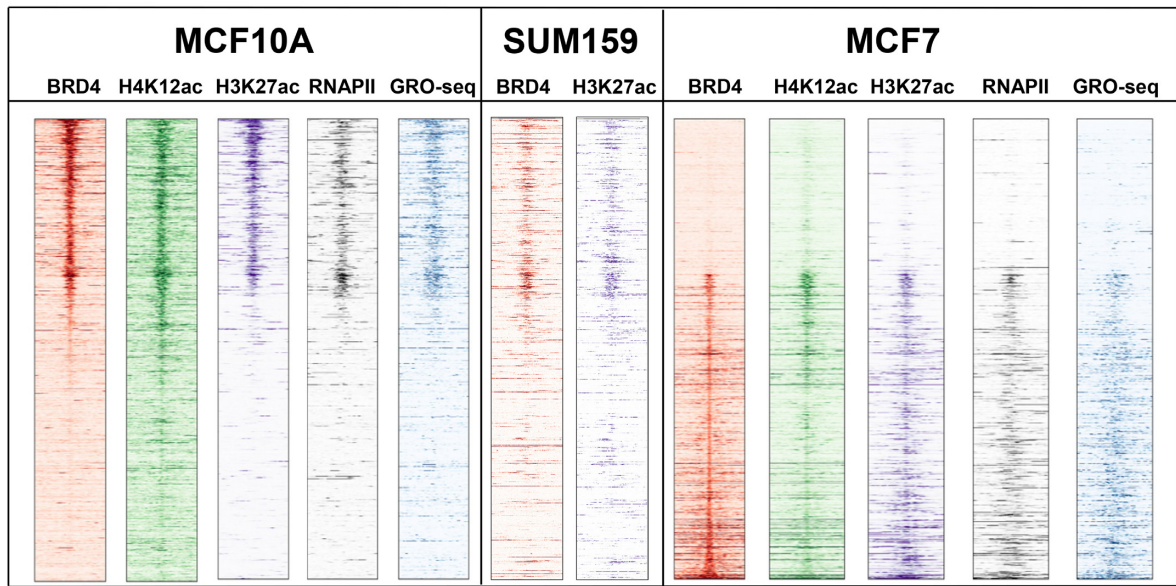
B

MSigDB_pathway_ID	Enrichment	HyperP	HyperFdrQ	TotalGenes
PID_A6B1_A6B4_INTEGRIN_PATHWAY	8.10E+00	7.29E-06	9.62E-03	46

| MSigDB_Perturbation_ID	Region Fold Enrichment	HyperP	Hyper FdrQ	TotalGenes
NAGASHIMA_EGF_SIGNALING_UP	1.17E+01	6.73E-07	1.89E-04	56
NAGASHIMA_NRG1_SIGNALING_UP	6.19E+00	1.51E-07	7.27E-05	168
AMIT_SERUM_RESPONSE_120_MCF10A	8.70E+00	2.31E-06	4.85E-04	63
LEONARD_HYPOXIA	1.38E+01	4.56E-04	2.32E-02	47
JAEGER_METASTASIS_DN	4.32E+00	7.01E-07	1.82E-04	254
SMID_BREAST_CANCER_BASAL_UP	2.72E+00	1.52E-04	1.07E-02	628
RICKMAN_METASTASIS_DN	5.34E+00	4.73E-04	2.37E-02	247

C
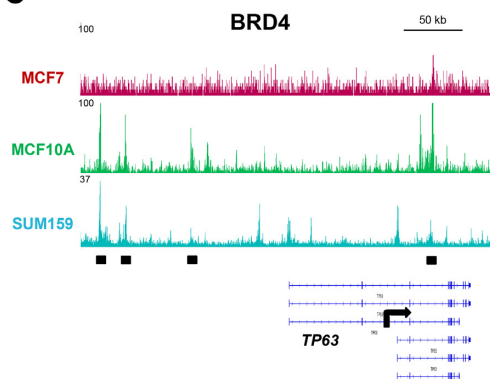
D
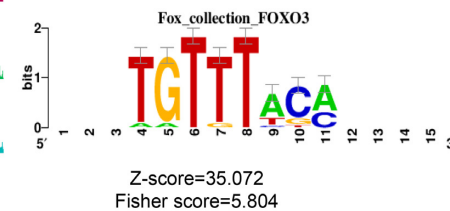
E
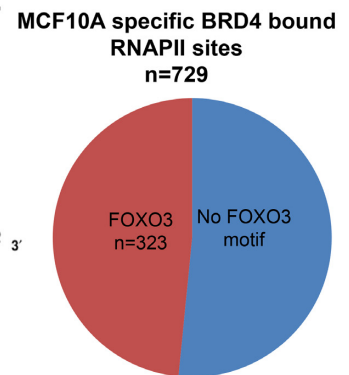
Figure 5. Basal epithelial cell context-specific BRD4-occupied distal regions are associated with FOXO factors. (**A**) Heatmap analyses depicting the occupancy of BRD4, H4K12ac, H3K27ac, RNAPII and enhancer RNA transcription shown by global run on sequencing (GRO-seq) on MCF10A and MCF7-specific distal BRD4-occupied regions identified by DiffBind analysis. BRD4 and H3K27ac occupancy is shown for SUM159 cells. (**B**) GREAT analyses on MCF10A-specific BRD4-occupied distal regions shows an enrichment of EGF and integrin-related pathways. FDR $\leq$ 0.05. "HyperP" denotes p-value, "HyperFdrQ" represents FDR q-value and "TotalGenes" represent total number of genes in the geneset. (**C**) Occupancy profiles of BRD4 from MCF7, MCF10A and SUM159 cells near the *TP63* gene. The active TSS and direction of transcription are indicated by the black arrow. Scale bar is shown in kilobases. MCF10A-specific enhancers shared with SUM159 are marked with black rectangles. (**D**) Motif analysis showing the enrichment of FOXO3 motif on MCF10A-specific distal BRD4 bound nucleosome-free regions. Z-score and Fisher scores are shown. (**E**) Distribution of FOXO3 motif-containing sites among the MCF10A-specific distal BRD4-occupied accessible chromatin regions.
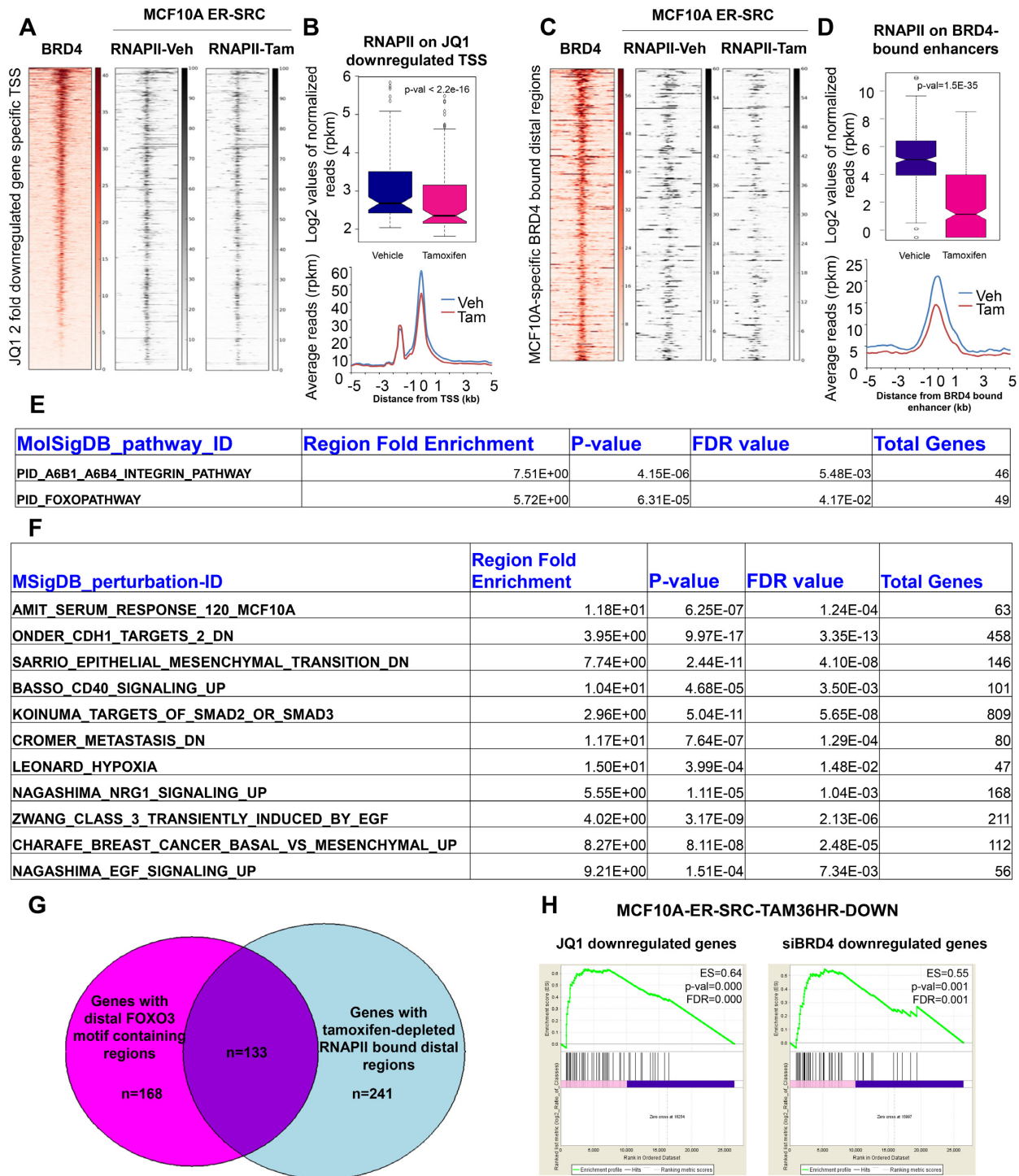
Figure 6. Association of BRD4 with Src signaling. (**A**, **C**) Heatmap analyses displaying the occupancy of BRD4 (MCF10A) and RNAPII under Vehicle (Veh) and Tamoxifen (Tam) treated conditions showing Src activity from MCF10A-ER-Src cells located around the TSS of genes downregulated by JQ1 (A) and at distal MCF10A-specific BRD4 occupied regions (C). Center represents TSS (A) or the distal site (C) and 5 kb upstream and downstream is shown. Scale depicts normalized RPKM values. (**B**, **D**) Boxplot and average profile showing the RNAPII occupancy in the presence or absence of Src activation located around TSS of the genes downregulated by JQ1 (B) and at MCF10A-specific BRD4 bound distal sites (D). Center represents TSS (B) or the distal site (D) and 5 kb upstream and downstream is shown. The plot shows the $\log_2$ values (box plot) and average (aggregate plot) normalized reads (in RPKM values) of RNAPII occupancy. (**E** and **F**) GREAT pathway analyses on differential regions with low occupancy of RNAPII following Src activation identified by DiffBind analyses. FDR $\leq$ 0.05. (**G**) Venn-diagram showing the overlap of genes associated with FOXO3 motif-containing MCF10A-specific distal BRD4 occupied regions and the genes associated with differential distal regions with low occupancy of RNAPII with Src activity as identified by GREAT analyses. (**H**) GSEA analyses showing enrichment plots comparing JQ1 and siBRD4 downregulated genes with the gene set downregulated upon Tamoxifen treatment for 36 hours in MCF10A-ER-Src cells (MCF10A-ER-Src-TAM36HR-DOWN). JQ1 or siBRD4 downregulated genes were arranged in ascending order of the $\log_2$ fold change. ES—enrichment score. *p*-val = *p*-value, FDR $\leq$ 0.05.
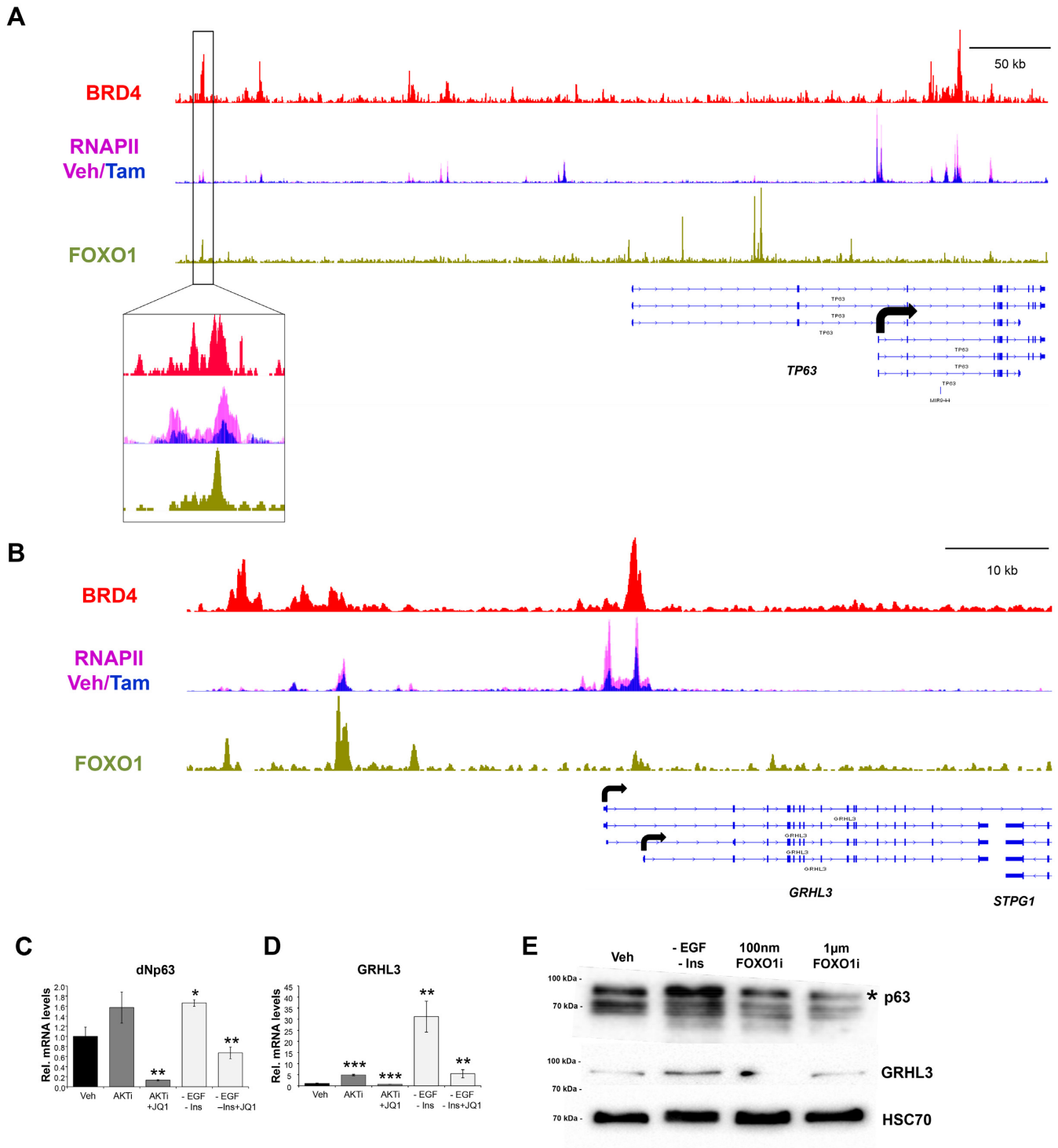
Figure 7. Association of BRD4 and EGF/AKT/FOXO signaling in the regulation of epithelial genes *TP63* and *GRHL3*. (**A** and **B**) Occupancy profiles of BRD4 (MCF10A), RNAPII under Vehicle (Veh) and Tamoxifen (Tam) treated conditions from MCF10A-ER-Src cells and FOXO1 from human endometrial stromal cells on distal regions of *TP63* (A) and *GRHL3* (B). The active TSS and direction of transcription are indicated by the black arrow. Scale bar is denoted in kb. (**C** and **D**) ΔNp63 (dNp63) (C) and *GRHL3* (D) expression in MCF10A cells regulated by administration of 10 μM AKT inhibitor (Perifosine, AKTi) and removal of EGF and Insulin (–EGF/–Ins) with or without JQ1 treatment for 24 h was confirmed by qPCR and denoted as 'Rel. mRNA levels'. Veh represents control MCF10A cells grown in DMEM/F12 media with EGF, insulin, cholera toxin and hydrocortisone. Data are represented as mean $\pm$ standard deviation. $n = 3$. ***$P \leq 0.001$, **$P \leq 0.01$, *$P \leq 0.05$. *P*-values were calculated using ANOVA single factor by comparing AKTi or –EGF/–Ins with Veh, AKTi+JQ1 with AKTi and –EGF/–Ins + JQ1 with –EGF/–Ins. (**E**) Western blot analyses of MCF10A protein lysates showing total p63 and GRHL3 expression with 100 nM and 1 μM of FOXO1 inhibitor AS1842856 (FOXO1i) for 24 h after removal of EGF and Insulin (-EGF/-Ins) for 48 h.

transcriptional activation, JQ1 treatment decreased the expression of established FOXO-regulated genes including *G6PC*, *PEPCK* and *MTTP*, where the effects of JQ1 mimicked those of insulin treatment (Supplementary Figure S7A). Consistently, ChIP-qPCR analyses showed that BRD4 occupies the previously published FOXO1-bound Insulin Response Element of *G6PC* (69), where treatment with either JQ1 or insulin decreased BRD4 occupancy on this region (Supplementary Figure S7B). Furthermore, administration of the FOXO1 inhibitor AS1842856 (25) partially blocked the induced expression of p63 and GRHL3 following the removal of EGF and Insulin (Figure 7E). Together these results suggest that activation of PI3K/AKT signaling in response to Src activation or growth factor signalling can affect basal epithelial cell phenotype by preventing FOXO/BRD4 activity at enhancers near genes such as *TP63* and *GRHL3*.

DISCUSSION

Transcriptional activation involves the complex association of various cofactors, epigenetic modifiers and chromatin remodelers to regulate a cell-specific gene expression programs. Maintenance of differentiation status requires a dynamic coordination of various transcription factors and epigenetic regulators in response to various stimuli. In this study, we show that the epigenetic reader BRD4 plays an important role in promoting a basal epithelial phenotype in non-transformed mammary cells by promoting RNAPII recruitment and eRNA production at distal regulatory regions occupied by the FOXO1 transcription factor proximal to genes such as *TP63* and *GRHL3*. Moreover, our findings strengthen the association between BRD4 and transcription factors with putative lineage-specifying enhancers.

Distal enhancers play an essential role in the regulation of cell type-specific gene transcription (70) where epigenetic regulation is tightly coupled with enhancer activity (71). Various studies highlight the central role of BRD4 in enhancer activity (6–9,26). This study reveals a specific association of BRD4 with distal regions of basal epithelial-specific genes. Furthermore, consistent with previous studies highlighting a mechanistic role of BRD4 in the regulation of enhancer activity (7,8), we also provide further evidence that BRD4 is a central regulator of enhancer RNA transcription. Together, our findings demonstrate an important function of BRD4 in determining epithelial cell characteristics by associating with enhancer regions and controlling their transcriptional activity.

p63 is an established marker for basal cells in the normal mammary epithelium where it plays an important role in epithelial development (59,60). In the normal mammary epithelium and in MCF10A cells, ΔNp63 is expressed at a higher level than TAp63 and plays an important role in the epithelial cell phenotype and survival (53,72), which resembles the function of BRD4 in our studies. Interestingly, p63 occupies cell-specific enhancer elements in keratinocytes where it is a central regulator of differentiation (73). More importantly, a recent study emphasized the importance of the p63 transcription factor network and its enhancer activation in the epigenetic status of mammary basal epithelial cell-specific lineage (22). *Grainy head*-like tran-

scription factors have also been widely investigated as tumor suppressors and recently discussed to be involved in the regulation of epidermal integrity, EMT and MET (74–78). Importantly, ectopic expression of a mesenchymal marker *SNAI2* resulted in the downregulation of *GRHL3* (79). Furthermore, a recent study shows that GRHL3 occupies the enhancer regions of the *CDH1* gene (encoding the epithelial marker E-Cadherin) and activates its expression, further supporting its role in controlling epithelial properties (58). Our findings uncover a previously unknown function of BRD4 in regulating *TP63* and *GRHL3* expression by associating with their distal enhancer regions, regulating the transcription of enhancer RNAs and presumably thereby regulating epithelial-associated gene expression. Thus, this supports the essential role of p63 and GRHL3 downstream of BRD4 in the regulation of epithelial differentiation.

The importance of BRD4 in controlling central lineage-specifying genes is well documented in different normal and cancer cell models and is related to its association with transcription factors on lineage-specific enhancers. BRD4 has been extensively characterized for its central role in promoting the expression of the MYC transcription factor as well as other genes important for cell proliferation and lineage specification (6,80,81). In embryonic stem cells, BRD4 inhibition affected stem cell maintenance, enhanced EMT and lead to neuro-ectodermal commitment by regulating the expression of stem cell markers and other transcription networks important for stem cell differentiation (82). The association of BRD4 with ERα in MCF7 breast luminal epithelial cancer cells (7) and TWIST in basal-like breast cancer cell lines (12) also provides substantial evidence that BRD4 is associated with lineage-specific transcription factors which are important for cell fate determination. Consistently, we and others have shown that BRD4 is required for osteoblast and osteoclast differentiation, where it regulates the transcription of cell-specific transcription factors, thereby determining cell fate decision (9,83–84). Specifically, we previously demonstrated that BRD4 cooperates with a network of transcription factors including C/EBPb, TEAD1, FOSL2 and JUND which function to recruit BRD4 to osteoblast-specific enhancers, which determine osteoblast differentiation and lineage specification (9). Our study further supports the importance of BRD4 in differentiation by uncovering its previously unknown role in normal epithelial differentiation in association with FOXO transcription factors.

In addition to its interaction with acetylated lysine residues on histones, recent studies have also demonstrated a direct association of BRD4 with transcription factors which play a vital role in cell-specific function and fate determination (12,85,86). It was proposed that the first bromodomain of BRD4 (BD1) may specifically associate with acetylated histones while the second bromodomain (BD2) can bind to acetylated lysine residues on cell-specific transcription factors (12,87). For example, one study showed that BRD4 interacts with acetylated lysine residues on histone-like motifs of these transcription factors (86). Interestingly, analyses of the amino acid sequences of FOXO1 and FOXO3 revealed similar histone-like motifs which were found to be acetylated in a curated mass spectrometry database (88) and could therefore potentially serve as di-

rect interacting sites for BRD4. This supports our findings that BRD4 and FOXO1 are co-localized to basal epithelial-specific enhancers and inactivation of FOXO factors in response to PI3K/AKT signaling results in a displacement of both FOXO and BRD4 from chromatin.

Overall our study suggests that a complex context-dependent hierarchy exists whereby BRD4-dependent cell type-specific gene expression can rapidly respond to intrinsic and extrinsic signals. Thus, we hypothesize that the clinical effectivity of BET inhibitors will largely depend on the context of individual signaling and transcription factor networks driven by oncogenic driver mutations. This study also suggests that caution should be maintained when administering BET domain inhibitors clinically since they may potentially promote unwanted cellular characteristics in certain contexts. Nevertheless, in mice injected with mammary epithelial tumors, BET inhibitors inhibited the primary cancer growth without increasing the incidence of metastatic breast tumors (15), suggesting that BET inhibitors indeed represent promising potential anti-tumor agents. A further understanding of the context-specific epigenetic function may help in further refining these inhibitors as potential therapeutic agents in various types of tumors.

ACCESSION NUMBERS

ChIP-seq and RNA-seq data described in this article are available in Gene Expression Omnibus under Accession numbers GSE72931 and GSE72932 respectively.

SUPPLEMENTARY DATA

Supplementary Data are available at NAR Online.

ACKNOWLEDGEMENTS

FUNDING

REFERENCES

1. Lee,T.I. and Young,R.A. (2013) Transcriptional Regulation and Its Misregulation in Disease. *Cell*, **152**, 1237–1251.
2. Peterlin,B.M. and Price,D.H. (2006) Controlling the elongation phase of transcription with P-TEFb. *Mol. Cell*, **23**, 297–305.
3. Yik,J.H., Chen,R., Nishimura,R., Jennings,J.L., Link,A.J. and Zhou,Q. (2003) Inhibition of P-TEFb (CDK9/Cyclin T) kinase and RNA polymerase II transcription by the coordinated actions of HEXIM1 and 7SK snRNA. *Mol. Cell*, **12**, 971–982.
4. Yang,Z., Yik,J.H.N., Chen,R., He,N., Jang,M.K., Ozato,K. and Zhou,Q. (2005) Recruitment of P-TEFb for stimulation of transcriptional elongation by the bromodomain protein Brd4. *Mol. Cell*, **19**, 535–545.
5. Filippakopoulos,P., Picaud,S., Mangos,M., Keates,T., Lambert,J.-P., Barsyte-Lovejoy,D., Felletar,I., Volkmer,R., Müller,S., Pawson,T. *et al.* (2012) Histone recognition and large-scale structural analysis of the human bromodomain family. *Cell*, **149**, 214–231.
6. Lovén,J., Hoke,H.A., Lin,C.Y., Lau,A., Orlando,D.A., Vakoc,C.R., Bradner,J.E., Lee,T.I. and Young,R.A. (2013) Selective inhibition of tumor oncogenes by disruption of super-enhancers. *Cell*, **153**, 320–334.
7. Nagarajan,S., Hossan,T., Alawi,M., Najafova,Z., Indenbirken,D., Bedi,U., Taipaleenmäki,H., Ben-Batalla,I., Scheller,M., Loges,S. *et al.* (2014) Bromodomain protein BRD4 is required for estrogen receptor-dependent enhancer activation and gene transcription. *Cell Rep.*, **8**, 460–469.
8. Kanno,T., Kanno,Y., LeRoy,G., Campos,E., Sun,H.-W., Brooks,S.R., Vahedi,G., Heightman,T.D., Garcia,B.A., Reinberg,D. *et al.* (2014) BRD4 assists elongation of both coding and enhancer RNAs by interacting with acetylated histones. *Nat. Struct. Mol. Biol.*, **21**, 1047–1057.
9. Najafova,Z., Tirado-Magallanes,R., Subramaniam,M., Hossan,T., Schmidt,G., Nagarajan,S., Baumgart,S.J., Mishra,V.K., Bedi,U., Hesse,E. *et al.* (2016) BRD4 localization to lineage-specific enhancers is associated with a distinct transcription factor repertoire. *Nucleic Acids Res.*, doi:10.1093/nar/gkw826.
10. Filippakopoulos,P. and Knapp,S. (2014) Targeting bromodomains: epigenetic readers of lysine acetylation. *Nat. Rev. Drug Discov.*, **13**, 337–356.
11. Feng,Q., Zhang,Z., Shea,M.J., Creighton,C.J., Coarfa,C., Hilsenbeck,S.G., Lanz,R., He,B., Wang,L., Fu,X. *et al.* (2014) An epigenomic approach to therapy for tamoxifen-resistant breast cancer. *Cell Res.*, **24**, 809–819.
12. Shi,J., Wang,Y., Zeng,L., Wu,Y., Deng,J., Zhang,Q., Lin,Y., Li,J., Kang,T., Tao,M. *et al.* (2014) Disrupting the interaction of BRD4 with diacetylated Twist suppresses tumorigenesis in basal-like breast cancer. *Cancer Cell*, **25**, 210–225.
13. Andrieu,G., Tran,A.H., Strissel,K.J. and Denis,G.V. (2016) BRD4 regulates breast cancer dissemination through Jagged1/Notch1 signaling. *Cancer Res.*, doi:10.1158/0008-5472.CAN-16-0559.
14. Crawford,N.P.S., Alsarraj,J., Lukes,L., Walker,R.C., Officewala,J.S., Yang,H.H., Lee,M.P., Ozato,K. and Hunter,K.W. (2008) Bromodomain 4 activation predicts breast cancer survival. *PNAS*, **105**, 6380–6385.
15. Alsarraj,J., Faraji,F., Geiger,T.R., Mattaini,K.R., Williams,M., Wu,J., Ha,N.-H., Merlino,T., Walker,R.C., Bosley,A.D. *et al.* (2013) BRD4 short isoform interacts with RRP1B, SIPA1 and components of the LINC complex at the inner face of the nuclear membrane. *PLoS ONE*, **8**, e80746.
16. Larue,L. and Bellacosa,A. (2005) Epithelial–mesenchymal transition in development and cancer: role of phosphatidylinositol 3′ kinase/AKT pathways. *Oncogene*, **24**, 7443–7454.
17. Zhuang,S., Duan,M. and Yan,Y. (2012) Src family kinases regulate renal epithelial dedifferentiation through activation of EGFR/PI3K signaling. *J. Cell Physiol.*, **227**, 2138–2144.
18. Normanno,N., De Luca,A., Bianco,C., Strizzi,L., Mancino,M., Maiello,M.R., Carotenuto,A., De Feo,G., Caponigro,F. and Salomon,D.S. (2006) Epidermal growth factor receptor (EGFR) signaling in cancer. *Gene*, **366**, 2–16.
19. Dansen,T.B. and Burgering,B.M.T. (2008) Unravelling the tumor-suppressive functions of FOXO proteins. *Trends Cell Biol.*, **18**, 421–429.

20. Wang,L., Brugge,J.S. and Janes,K.A. (2011) Intersection of FOXO- and RUNX1-mediated gene expression programs in single breast epithelial cells during morphogenesis and tumor progression. *Proc. Natl. Acad. Sci. U.S.A.*, **108**, E803–E812.

21. Matkar,S., Sharma,P., Gao,S., Gurung,B., Katona,B.W., Liao,J., Muhammad,A.B., Kong,X.-C., Wang,L., Jin,G. *et al.* (2015) An epigenetic pathway regulates sensitivity of breast cancer cells to HER2 inhibition via FOXO/c-Myc axis. *Cancer Cell*, **28**, 472–485.

22. Pellacani,D., Bilenky,M., Kannan,N., Heravi-Moussavi,A., Knapp,D.J.H.F., Gakkhar,S., Moksa,M., Carles,A., Moore,R., Mungall,A.J. *et al.* (2016) Analysis of normal human mammary epigenomes reveals cell-specific active enhancer states and associated transcription factor networks. *Cell Rep.*, **17**, 2060–2074.

23. Bedi,U., Scheel,A.H., Hennion,M., Begus-Nahrmann,Y., Rüschoff,J. and Johnsen,S.A. (2014) SUPT6H controls estrogen receptor activity and cellular differentiation by multiple epigenomic mechanisms. *Oncogene*, doi:10.1038/onc.2013.558.

24. Smalley,M.J. (2010) Isolation, culture and analysis of mouse mammary epithelial cells. *Methods Mol. Biol.*, **633**, 139–170.

25. Nagashima,T., Shigematsu,N., Maruki,R., Urano,Y., Tanaka,H., Shimaya,A., Shimokawa,T. and Shibasaki,M. (2010) Discovery of novel forkhead box O1 inhibitors for treating type 2 diabetes: improvement of fasting glycemia in diabetic db/db mice. *Mol. Pharmacol.*, **78**, 961–970.

26. Nagarajan,S., Benito,E., Fischer,A. and Johnsen,S.A. (2015) H4K12ac is regulated by estrogen receptor-alpha and is associated with BRD4 function and inducible transcription. *Oncotarget*, **6**, 7305–7317.

27. Kim,Y.J., Greer,C.B., Cecchini,K.R., Harris,L.N., Tuck,D.P. and Kim,T.H. (2013) HDAC inhibitors induce transcriptional repression of high copy number genes in breast cancer through elongation blockade. *Oncogene*, **32**, 2828–2835.

28. Vasquez,Y.M., Mazur,E.C., Li,X., Kommagani,R., Jiang,L., Chen,R., Lanz,R.B., Kovanci,E., Gibbons,W.E. and DeMayo,F.J. (2015) FOXO1 is required for binding of PR on IRF4, novel transcriptional regulator of endometrial stromal decidualization. *Mol. Endocrinol.*, **29**, 421–433.

29. Shu,S., Lin,C.Y., He,H.H., Witwicki,R.M., Tabassum,D.P., Roberts,J.M., Janiszewska,M., Huh,S.J., Liang,Y., Ryan,J. *et al.* (2016) Response and resistance to BET bromodomain inhibitors in triple-negative breast cancer. *Nature*, **529**, 413–417.

30. Welboren,W.-J., van Driel,M.A., Janssen-Megens,E.M., van Heeringen,S.J., Sweep,F.C., Span,P.N. and Stunnenberg,H.G. (2009) ChIP-Seq of ERalpha and RNA polymerase II defines genes differentially responding to ligands. *EMBO J.*, **28**, 1418–1428.

31. Hah,N., Murakami,S., Nagari,A., Danko,C.G. and Kraus,W.L. (2013) Enhancer transcripts mark active estrogen receptor binding sites. *Genome Res.*, **23**, 1210–1223.

32. Joseph,R., Orlov,Y.L., Huss,M., Sun,W., Kong,S.L., Ukil,L., Pan,Y.F., Li,G., Lim,M., Thomsen,J.S. *et al.* (2010) Integrative model of genomic factors for determining binding site selection by estrogen receptor-α;. *Mol. Syst. Biol.*, **6**, 456.

33. Theodorou,V., Stark,R., Menon,S. and Carroll,J.S. (2013) GATA3 acts upstream of FOXA1 in mediating ESR1 binding by shaping enhancer accessibility. *Genome Res.*, **23**, 12–22.

34. Ross-Innes,C.S., Stark,R., Teschendorff,A.E., Holmes,K.A., Ali,H.R., Dunning,M.J., Brown,G.D., Gojis,O., Ellis,I.O., Green,A.R. *et al.* (2012) Differential oestrogen receptor binding is associated with clinical outcome in breast cancer. *Nature*, **481**, 389–393.

35. Ho Sui,S.J., Fulton,D.L., Arenillas,D.J., Kwon,A.T. and Wasserman,W.W. (2007) oPOSSUM: integrated tools for analysis of regulatory motif over-representation. *Nucleic Acids Res.*, **35**, W245–W252.

36. McLean,C.Y., Bristor,D., Hiller,M., Clarke,S.L., Schaar,B.T., Lowe,C.B., Wenger,A.M. and Bejerano,G. (2010) GREAT improves functional interpretation of cis-regulatory regions. *Nat. Biotechnol.*, **28**, 495–501.

37. Langmead,B. and Salzberg,S.L. (2012) Fast gapped-read alignment with Bowtie 2. *Nat. Methods*, **9**, 357–359.

38. Anders,S. and Huber,W. (2010) Differential expression analysis for sequence count data. *Genome Biol.*, **11**, R106.

39. Subramanian,A., Tamayo,P., Mootha,V.K., Mukherjee,S., Ebert,B.L., Gillette,M.A., Paulovich,A., Pomeroy,S.L., Golub,T.R.,

Lander,E.S. *et al.* (2005) Gene set enrichment analysis: a knowledge-based approach for interpreting genome-wide expression profiles. *Proc. Natl. Acad. Sci. U.S.A.*, **102**, 15545–15550.

40. Liberzon,A., Subramanian,A., Pinchback,R., Thorvaldsdóttir,H., Tamayo,P. and Mesirov,J.P. (2011) Molecular signatures database (MSigDB) 3.0. *Bioinformatics*, **27**, 1739–1740.

41. Bosco,A., Ehteshami,S., Stern,D.A. and Martinez,F.D. (2010) Decreased activation of inflammatory networks during acute asthma exacerbations is associated with chronic airflow obstruction. *Mucosal Immunol.*, **3**, 399–409.

42. Manalo,D.J., Rowan,A., Lavoie,T., Natarajan,L., Kelly,B.D., Ye,S.Q., Garcia,J.G.N. and Semenza,G.L. (2005) Transcriptional regulation of vascular endothelial cell responses to hypoxia by HIF-1. *Blood*, **105**, 659–669.

43. Wong,D.J., Liu,H., Ridky,T.W., Cassarino,D., Segal,E. and Chang,H.Y. (2008) Module map of stem cell genes guides creation of epithelial cancer stem cells. *Cell Stem Cell*, **2**, 333–344.

44. Cromer,A., Carles,A., Millon,R., Ganguli,G., Chalmel,F., Lemaire,F., Young,J., Dembélé,D., Thibault,C., Muller,D. *et al.* (2004) Identification of genes associated with tumorigenesis and metastatic potential of hypopharyngeal cancer by microarray analysis. *Oncogene*, **23**, 2484–2498.

45. Sotiriou,C., Wirapati,P., Loi,S., Harris,A., Fox,S., Smeds,J., Nordgren,H., Farmer,P., Praz,V., Haibe-Kains,B. *et al.* (2006) Gene expression profiling in breast cancer: understanding the molecular basis of histologic grade to improve prognosis. *J. Natl. Cancer Inst.*, **98**, 262–272.

46. Lin,H.-J.L., Zuo,T., Lin,C.-H., Kuo,C.T., Liyanarachchi,S., Sun,S., Shen,R., Deatherage,D.E., Potter,D., Asamoto,L. *et al.* (2008) Breast cancer-associated fibroblasts confer AKT1-mediated epigenetic silencing of Cystatin M in epithelial cells. *Cancer Res.*, **68**, 10257–10266.

47. Jaeger,J., Koczan,D., Thiesen,H.-J., Ibrahim,S.M., Gross,G., Spang,R. and Kunz,M. (2007) Gene expression signatures for tumor progression, tumor subtype, and tumor thickness in laser-microdissected melanoma tissues. *Clin. Cancer Res.*, **13**, 806–815.

48. O'Donnell,R.K., Kupferman,M., Wei,S.J., Singhal,S., Weber,R., O'Malley,B., Cheng,Y., Putt,M., Feldman,M., Ziober,B. *et al.* (2005) Gene expression signature predicts lymphatic metastasis in squamous cell carcinoma of the oral cavity. *Oncogene*, **24**, 1244–1251.

49. Charafe-Jauffret,E., Ginestier,C., Monville,F., Finetti,P., Adélaïde,J., Cervera,N., Fekairi,S., Xerri,L., Jacquemier,J., Birnbaum,D. *et al.* (2006) Gene expression profiling of breast cell lines identifies potential new basal markers. *Oncogene*, **25**, 2273–2284.

50. Huang,D.W., Sherman,B.T. and Lempicki,R.A. (2008) Systematic and integrative analysis of large gene lists using DAVID bioinformatics resources. *Nat. Protocols*, **4**, 44–57.

51. Hirsch,H.A., Iliopoulos,D., Joshi,A., Zhang,Y., Jaeger,S.A., Bulyk,M., Tsichlis,P.N., Shirley Liu,X. and Struhl,K. (2010) A transcriptional signature and common gene networks link cancer with lipid metabolism and diverse human diseases. *Cancer Cell*, **17**, 348–361.

52. Gautier,L., Cope,L., Bolstad,B.M. and Irizarry,R.A. (2004) affy—analysis of Affymetrix GeneChip data at the probe level. *Bioinformatics*, **20**, 307–315.

53. Carroll,D.K., Carroll,J.S., Leong,C.-O., Cheng,F., Brown,M., Mills,A.A., Brugge,J.S. and Ellisen,L.W. (2006) p63 regulates an adhesion programme and cell survival in epithelial cells. *Nat Cell Biol.*, **8**, 551–561.

54. Subramanian,A., Tamayo,P., Mootha,V.K., Mukherjee,S., Ebert,B.L., Gillette,M.A., Paulovich,A., Pomeroy,S.L., Golub,T.R., Lander,E.S. *et al.* (2005) Gene set enrichment analysis: a knowledge-based approach for interpreting genome-wide expression profiles. *Proc. Natl. Acad. Sci. U.S.A.*, **102**, 15545–15550.

55. Chirivi,R.G.S., Garofalo,A., Padura,I.M., Mantovani,A. and Giavazzi,R. (1993) Interleukin 1 receptor antagonist inhibits the augmentation of metastasis induced by interleukin 1 or lipopolysaccharide in a human melanoma/nude mouse system. *Cancer Res.*, **53**, 5051–5054.

56. Oliver,J.R., Kushwah,R. and Hu,J. (2012) Multiple roles of the epithelium-specific ETS transcription factor, ESE-1, in development and disease. *Lab. Invest.*, **92**, 320–330.

57. Ting,S.B., Caddy,J., Hislop,N., Wilanowski,T., Auden,A., Zhao,L.-L., Ellis,S., Kaur,P., Uchida,Y., Holleran,W.M. *et al.* (2005) A homolog of Drosophila grainy head is essential for epidermal integrity in mice. *Science*, **308**, 411–413.

58. Alotaibi,H., Basilicata,M.F., Shehwana,H., Kosowan,T., Schreck,I., Braeutigam,C., Konu,O., Brabletz,T. and Stemmler,M.P. (2015) Enhancer cooperativity as a novel mechanism underlying the transcriptional regulation of E-cadherin during mesenchymal to epithelial transition. *Biochim. Biophys. Acta*, **1849**, 731–742.

59. Yang,A., Schweitzer,R., Sun,D., Kaghad,M., Walker,N., Bronson,R.T., Tabin,C., Sharpe,A., Caput,D., Crum,C. *et al.* (1999) p63 is essential for regenerative proliferation in limb, craniofacial and epithelial development. *Nature*, **398**, 714–718.

60. Nylander,K., Vojtesek,B., Nenutil,R., Lindgren,B., Roos,G., Zhanxiang,W., Sjöström,B., Dahlqvist,Å. and Coates,P.J. (2002) Differential expression of p63 isoforms in normal tissues and neoplastic cells. *J. Pathol.*, **198**, 417–427.

61. Villafane,B. and Sebastian,J. (2012) *Role of P63 in cell migration and cancer metastasis*. Boston University, Ann Arbor.

62. Maschler,S., Wirl,G., Spring,H., Bredow,D.V., Sordat,I., Beug,H. and Reichmann,E. (2005) Tumor cell invasiveness correlates with changes in integrin expression and localization. *Oncogene*, **24**, 2032–2041.

63. Lamb,L.E., Zarif,J.C. and Miranti,C.K. (2011) The androgen receptor induces integrin α6β1 to promote prostate tumor cell survival via NF-κB and Bcl-xL Independently of PI3K signaling. *Cancer Res.*, **71**, 2739–2749.

64. Hood,J.D. and Cheresh,D.A. (2002) Role of integrins in cell invasion and migration. *Nat. Rev. Cancer*, **2**, 91–100.

65. Schmoll,D., Walker,K.S., Alessi,D.R., Grempler,R., Burchell,A., Guo,S., Walther,R. and Unterman,T.G. (2000) Regulation of glucose-6-phosphatase gene expression by protein kinase Balpha and the forkhead transcription factor FKHR. Evidence for insulin response unit-dependent and -independent effects of insulin on promoter activity. *J. Biol. Chem.*, **275**, 36324–36333.

66. Nakae,J., Kitamura,T., Silver,D.L. and Accili,D. (2001) The forkhead transcription factor Foxo1 (Fkhr) confers insulin sensitivity onto glucose-6-phosphatase expression. *J. Clin. Invest.*, **108**, 1359–1367.

67. Samuel,V.T., Choi,C.S., Phillips,T.G., Romanelli,A.J., Geisler,J.G., Bhanot,S., McKay,R., Monia,B., Shutter,J.R., Lindberg,R.A. *et al.* (2006) Targeting foxo1 in mice using antisense oligonucleotide improves hepatic and peripheral insulin action. *Diabetes*, **55**, 2042–2050.

68. Kamagate,A., Qu,S., Perdomo,G., Su,D., Kim,D.H., Slusher,S., Meseck,M. and Dong,H.H. (2008) FoxO1 mediates insulin-dependent regulation of hepatic VLDL production in mice. *J. Clin. Invest.*, **118**, 2347–2364.

69. Singh,B.K., Sinha,R.A., Zhou,J., Xie,S.Y., You,S.-H., Gauthier,K. and Yen,P.M. (2013) FoxO1 Deacetylation regulates thyroid hormone-induced transcription of key hepatic gluconeogenic genes. *J. Biol. Chem.*, **288**, 30365–30372.

70. Ong,C.-T. and Corces,V.G. (2011) Enhancer function: new insights into the regulation of tissue-specific gene expression. *Nat. Rev. Genet.*, **12**, 283–293.

71. Heintzman,N.D., Hon,G.C., Hawkins,R.D., Kheradpour,P., Stark,A., Harp,L.F., Ye,Z., Lee,L.K., Stuart,R.K., Ching,C.W. *et al.* (2009) Histone modifications at human enhancers reflect global cell-type-specific gene expression. *Nature*, **459**, 108–112.

72. Lindsay,J., McDade,S.S., Pickard,A., McCloskey,K.D. and McCance,D.J. (2011) Role of DeltaNp63gamma in epithelial to mesenchymal transition. *J. Biol. Chem.*, **286**, 3915–3924.

73. Cavazza,A., Miccio,A., Romano,O., Petiti,L., Malagoli Tagliazucchi,G., Peano,C., Severgnini,M., Rizzi,E., De Bellis,G., Bicciato,S. *et al.* (2016) Dynamic transcriptional and epigenetic regulation of human epidermal keratinocyte differentiation. *Stem Cell Rep.*, **6**, 618–632.

74. Ting,S.B., Caddy,J., Hislop,N., Wilanowski,T., Auden,A., Zhao,L.-L., Ellis,S., Kaur,P., Uchida,Y., Holleran,W.M. *et al.* (2005) A homolog of Drosophila grainy head is essential for epidermal integrity in mice. *Science*, **308**, 411–413.

75. Darido,C., Georgy,S.R., Wilanowski,T., Dworkin,S., Auden,A., Zhao,Q., Rank,G., Srivastava,S., Finlay,M.J., Papenfuss,A.T. *et al.* (2011) Targeting of the tumor suppressor GRHL3 by a miR-21-dependent proto-oncogenic network results in PTEN loss and tumorigenesis. *Cancer Cell*, **20**, 635–648.

76. Cieply,B., Riley,P., Pifer,P.M., Widmeyer,J., Addison,J.B., Ivanov,A.V., Denvir,J. and Frisch,S.M. (2012) Suppression of the epithelial–mesenchymal transition by grainyhead-like-2. *Cancer Res.*, **72**, 2440–2453.

77. Frisch,S.M., Schaller,M. and Cieply,B. (2013) Mechanisms that link the oncogenic epithelial–mesenchymal transition to suppression of anoikis. *J Cell Sci*, **126**, 21–29.

78. Werner,S., Frey,S., Riethdorf,S., Schulze,C., Alawi,M., Kling,L., Vafaizadeh,V., Sauter,G., Terracciano,L., Schumacher,U. *et al.* (2013) Dual Roles of the Transcription Factor Grainyhead-like 2 (GRHL2) in Breast Cancer. *J. Biol. Chem.*, **288**, 22993–23008.

79. Mistry,D.S., Chen,Y., Wang,Y., Zhang,K. and Sen,G.L. (2014) SNAI2 controls the undifferentiated state of human epidermal progenitor cells. *Stem Cells*, **32**, 3209–3218.

80. Chapuy,B., McKeown,M.R., Lin,C.Y., Monti,S., Roemer,M.G.M., Qi,J., Rahl,P.B., Sun,H.H., Yeda,K.T., Doench,J.G. *et al.* (2013) Discovery and characterization of super-enhancer-associated dependencies in diffuse large B cell lymphoma. *Cancer Cell*, **24**, 777–790.

81. Delmore,J.E., Issa,G.C., Lemieux,M.E., Rahl,P.B., Shi,J., Jacobs,H.M., Kastritis,E., Gilpatrick,T., Paranal,R.M., Qi,J. *et al.* (2011) BET bromodomain inhibition as a therapeutic strategy to target c-Myc. *Cell*, **146**, 904–917.

82. Micco,R.D., Fontanals-Cirera,B., Low,V., Ntziachristos,P., Yuen,S.K., Lovell,C.D., Dolgalev,I., Yonekubo,Y., Zhang,G., Rusinova,E. *et al.* (2014) Control of embryonic stem cell identity by BRD4-dependent transcriptional elongation of super-enhancer-associated pluripotency genes. *Cell Rep.*, **9**, 234–247.

83. Lamoureux,F., Baud'huin,M., Rodriguez Calleja,L., Jacques,C., Berreur,M., Rédini,F., Lecanda,F., Bradner,J.E., Heymann,D. and Ory,B. (2014) Selective inhibition of BET bromodomain epigenetic signalling interferes with the bone-associated tumour vicious cycle. *Nat. Commun.*, **5**, 3511.

84. Baud'huin,M., Lamoureux,F., Jacques,C., Rodriguez Calleja,L., Quillard,T., Charrier,C., Amiaud,J., Berreur,M., Brounais-LeRoyer,B., Owen,R. *et al.* (2017) Inhibition of BET proteins and epigenetic signaling as a potential treatment for osteoporosis. *Bone*, **94**, 10–21.

85. Wu,S.-Y., Lee,A.-Y., Lai,H.-T., Zhang,H. and Chiang,C.-M. (2013) Phospho switch triggers Brd4 chromatin binding and activator recruitment for gene-specific targeting. *Mol. Cell*, **49**, 843–857.

86. Roe,J.-S., Mercan,F., Rivera,K., Pappin,D.J. and Vakoc,C.R. (2015) BET bromodomain inhibition suppresses the function of hematopoietic transcription factors in acute myeloid leukemia. *Mol. Cell*, **58**, 1028–1039.

87. Shi,J. and Vakoc,C.R. (2014) The mechanisms behind the therapeutic activity of BET bromodomain inhibition. *Mol. Cell*, **54**, 728–736.

88. Hornbeck,P.V., Zhang,B., Murray,B., Kornhauser,J.M., Latham,V. and Skrzypek,E. (2015) PhosphoSitePlus, 2014: mutations, PTMs and recalibrations. *Nucleic Acids Res.*, **43**, D512–D520.